Exploring the Material Properties of Small Scale Folded Structures
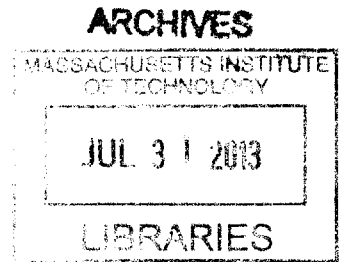
by

Megan E. Uberti

Submitted to the
Department of Mechanical Engineering
in Partial Fulfillment of the Requirements for the Degree of

Bachelor of Science in Mechanical Engineering

at the

Massachusetts Institute of Technology

June 2013

Signature of Author: _____
Department of Mechanical Engineering
May 10, 2013

Certified by: _____
Daniela Rus
Professor of Electrical Engineering and Computer Science
Thesis Supervisor

Accepted by: _____
Anette Hosoi
Professor of Mechanical Engineering
Undergraduate Officer

Exploring the Material Properties of Small Scale Folded Structures

by

Megan E. Uberti

Submitted to the Department of Mechanical Engineering
on May 10, 2013 in Partial Fulfillment of the
Requirements for the Degree of

Bachelor of Science in Mechanical Engineering

ABSTRACT

The printable robotics project makes use of fast and inexpensive 2D fabrication technologies to make robotics more readily available to the average person. Although designs for a number of successful printable robots have already been produced, there has been little formal exploration into the materials properties of these structures. Three point bending tests were performed on beams made of the materials and cross-sectional geometries of current designs to determine the bending stiffness of the printable beams currently found in printable robots, particularly the printable quad-rotor frame. As expected the composite acrylic and PEEK triangular beam had the highest bending stiffness EI at 4.15 ± 1.67 N*m^2. The lowest EI was the triangular PEEK beam in its weak configuration at 0.02 ± 0.005 N*m^2. 3D printed ABS beams had an unreliable result, with EI in the range of 11.7 ± 8.05 N*m^2. Overall our experimentally calculated values for EI were generally consistent with the theoretically calculated values, providing useful information to inform future design choices and understanding the limitations of printable robot structures.

Thesis Supervisor: Daniela Rus
Title: Professor of Electrical Engineering and Computer Science
       Director, CSAIL

ACKNOWLEDGEMENTS

TABLE OF CONTENTS

INTRODUCTION

Traditionally, the fabrication of robotic systems has required expensive and specialized processes as well as in-depth technical knowledge. The goal of the printable robotics project is to significantly reduce the cost and time necessary to build a robot, as well as make these processes available to users with little technical expertise.

Using fast and inexpensive 2D fabrication techniques and an "origami-inspired" approach, laser-cut sheets of thin plastic with copper-etched circuits can be folded into 3D, fully functional robots [1]. This "origami-inspired" approach allows for rapid and low-cost manufacturing of robots, and also makes robotics more readily available to users at home.

Ultimately, the goal of this project is for a user at home to specify a desired task, such as a robot that can fly and carry a specified payload, and then input this high-level design criterion to a printable robot compiler, which would then produce an appropriate design from an existing database of component parts. To reach this goal, this database must be pre-populated with component designs which the compiler can draw from. Already designs for insect-like crawling robots and a robotic gripper arm exist, and we plan to continue adding mechanical and electrical designs for expanded possibilities in function for printable robotics.

BACKGROUND

Manufacturing of Printable Robots

Our approach to manufacturing printable robots begins with a 2D sheet of thin polymer. After the design for a robot is drawn using CAD software, the pattern is sent to a laser cutter to be cut onto the thin polymer sheet. Dotted lines are cut as guides for folding the robot into its final 3D structure and tab and slot features are used to hold edges securely together.

Next a piece of copper tape is mounted onto the PEEK and an electrical circuit is printed in black ink on top of the copper. A ferric chloride etcher is used to etch away the exposed copper, leaving only the traces masked by the black ink. Electrical components are then soldered onto the board by hand, although the use of pick-and-place machines has been considered to eliminate the need for hand soldering in the future. In many of our current designs, an ATTiny13A microprocessor has been used to control the actuators on the robot. This is soldered on and programmed on the board through a six-pin programming cable and an Atmel STK500 programming board.
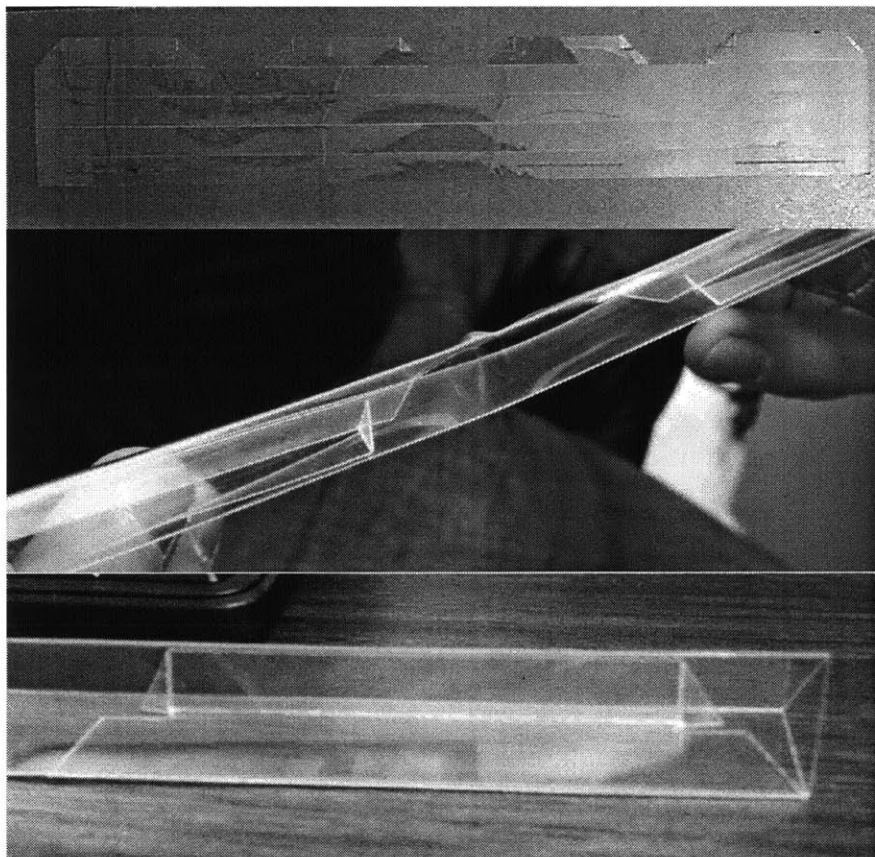

Figure 1: Top) A 2D sheet of polyester which has been cut into a printable robot template using a Versa laser cutter. Perforated lines are used as guides for folding. Middle) The folded beam

made from the above template. Bottom) Close-up of the tab and slot feature used to hold two faces together.

Materials Properties of "Origami" Robots

Previously PEEK (poly ether ether ketone) was the material of choice for the bodies of printable robots because of its durability and heat-resistant properties. The value of Young's modulus E given by the manufacturer is 3.6 GPa [6]. However, as new printable robot designs are being constructed, concerns such as cost and material strength have arose. PEEK is expensive compared to alternative polymer sheets, and the material naturally does not provide any rigidity or stiffness.

One alternative is thin polyester, sold in sheet form, which has similar properties to PEEK but is less expensive. The Young's modulus given by the manufacturer for polyester ranges from 3GPa to 4GPa [7], so we used 3.5GPa in our calculations.

Another alternative is a composite material using an acrylic skeleton wrapped in a PEEK skin. The acrylic pieces are cut with the laser cutter, and snap together using matching notches along the edges. Adhesive-backed PEEK is then wrapped around the entire structure, providing additional strength as well as creating a continuous surface for the copper circuits to be etched onto.

Another but less successful method was to fill the thin polymer structures with hardening spray foam, but this was messy and very difficult to achieve even filling, resulting in discontinuities in the material. Although these structures were noticeably more resilient, the complications in manufacturing made it an unfavorable choice.

Previous work on a jumping printable robot proved difficult because of the lack of stiffness inherent in the thin polymer sheets used for robot body construction. More recently, work on a printable quad-rotor flying robot has created a need to quantify the material properties of printable robots. Ideally, the printable robot compiler would be able to take high level design criteria, such as a quad rotor that can carry a payload up to 100 grams, and create a robot body design from the existing component designs in the database. The quad-rotor frames must be lightweight enough to fly, but must also have sufficient stiffness to carry the specified load without bending or breaking.

In a larger context, understanding the bending stiffness of printable structures will be helpful for creating new designs as well as improving the capability of the software used for producing the design templates. Although values for Young's modulus are available for most materials, and moment of inertia I can be calculated analytically, we would like to explore if these values hold true for these small scale, thin, folded structures.

It is also important to note that material stiffness is not the only consideration in these tests. We must also consider cost, the time required to manufacture, and the ease of manufacturing. Time to manufacture refers to the time required to procure materials and laser cut the template, while ease of manufacture will refer to the time required to fold the piece by hand, as well as any additional layers of complexity, such as using an adhesive to assemble.

Beam Stiffness

Beam stiffness can be calculated by performing a three point bending test on representative printable beams. The three point bending test is a popular and well-known method in materials testing [2]. In the three point bending test, a point force is applied to the center of a

beam simply supported at both ends. The force is measured using a sensor, and the maximum deflection, which occurs at the midpoint of the beam, is measured.
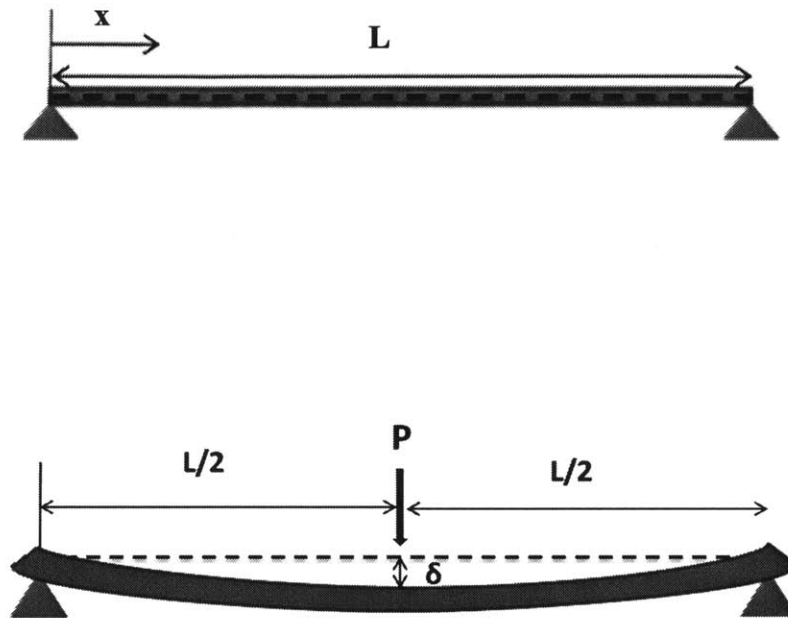

Figure 2: Top) Diagram of a beam simply supported at both ends. Total length is L and position x is measured from the left end. Bottom) A load P is applied at the midpoint of the beam, inducing a deflection δ of the midpoint.

For a beam simply supported at both ends with a point force applied in the middle, the beam equation can be derived as follows [2],

$$M(x) = EIv''(x) \tag{1}$$

Where M(x) is the moment equation, E is the Young's modulus, I is the area moment of inertia, and v(x) is the deflection of the beam. Applying a moment balance to the beam, we see that,

13

$$M(x) = \frac{P}{2}x - P(x - \frac{L}{2}) \qquad (2)$$

Using this expression for M(x) and integrating once,

$$EIv'(x) = \frac{P}{4}x^2 - \frac{P}{2}\left(x - \frac{L}{2}\right)^2 + c_1 \qquad (3)$$

Integrating again,

$$EIv(x) = \frac{P}{12}x^3 - \frac{P}{6}\left(x - \frac{L}{2}\right)^3 - c_1 x + c_2 \qquad (4)$$

To solve for the constants, we apply boundary conditions: v'(x) = 0 at x = L/2 and v(x) = 0 at x = 0. This gives us,

$$c_1 = -\frac{PL^2}{16} \; ; \; c_2 = 0 \qquad (5)$$

Plugging in these values and rearranging so that v(x) is isolated,

$$v(x) = \frac{P}{48EI}\left(4x^3 - 3L^2 x - 8\left(x - \frac{L}{2}\right)^3\right) \qquad (6)$$

The maximum deflection occurs at x = L/2, the midpoint of the beam. Plugging in this value, we can find an expression for max deflection in terms of load applied P, length of the beam L, Young's modulus E, and moment of inertia I,

14

$$\delta_{max} = \frac{PL^3}{48EI} \qquad (7)$$

In beam bending, the value of EI is referred to as the beam stiffness, or flexural rigidity. Experimentally we will measure P and δ so that we can find the value of EI for our printable folded structures, and then analyze whether our theoretical values for E and I were accurate at this scale. E can generally be obtained from a table or from the manufacturer of the material, and I can be calculated analytically [3].

The moment of inertia for square cross-sections is,

$$I = \frac{b^4}{12} \qquad (8)$$

Where b is the length of a side. Moment of inertia for a triangular cross-section is,

$$I = \frac{bh^3}{36} \qquad (9)$$

Where b is the length of the base and h is the height, with respect to an axis through the centroid. The printable beams are hollow, so we will use the following approach to calculate moment of inertia,

$$I_{total} = I_{outer} - I_{inner}$$

EXPERIMENTAL DESIGN

Three Point Bending Test Setup

For the testing, a Totalcomp TS-26 S-type load cell [4]was attached to a vertical support which was clamped to the lab table. Two solid cylinders resting in holders supported the ends of the beam one-quarter of the beam's total length from each end. The cylinders supported the beam while also creating an essentially frictionless surface for the beam to move while it deformed.

A USB 1608fs from Measurement Computing was used to collect the data [5], and a LabVIEW program was used to visualize the data.
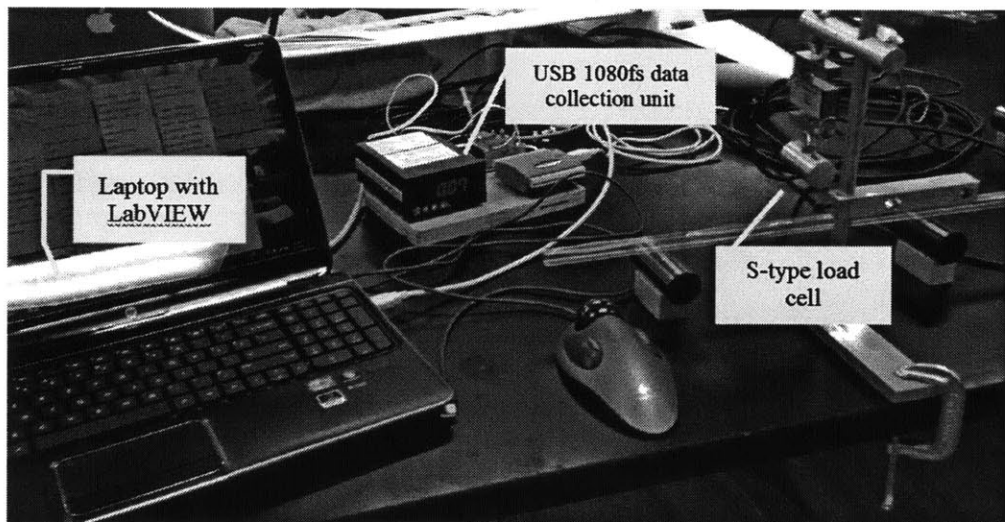

Figure 3: Picture of the experimental setup. An S-type load cell was applied at the midpoint of a beam simply supported at both ends. Data was collected with a Measurement Computing USB 1080fs unit and analyzed using LabVIEW software.

Data Collection Procedure

For the three point bending method to be accurate and effective, it is best to use test specimens that are long and thin. Representative beams of similar cross-sections to those used in current printable robot designs were fabricated at a 500 mm length (with the exception of the 3D printed beams, which were limited by the capacity of the 3D printer to only 240 mm). The beam was then placed into our test apparatus, with the midpoint of the beam directly underneath the force sensor. The beam was supported by solid cylinders at one-quarter distance from each end. Then the force sensor would be slowly lowered until it was contacting the beam and slight vertical displacement was noticeable. Applying too great a deflection, or applying a deflection too quickly, can create unreliable data, especially if a plastic deformation was induced in the beam.

After the force is applied, the force (in Newton) could be read from the digital readout of a USB 1608fs unit from Measurement Computing. The deflection (in mm) at the midpoint of the beam was also recorded. Each specimen was tested at least three times.

RESULTS AND DISCUSSION

TEST SPECIMEN	EI experimental [N*m^2]	EI calculated [N*m^2]
Polyester .010" Square	0.64 ± 0.15	0.30
Polyester .005" Square	0.35 ± 0.06	0.15
PEEK Triangle	0.07 ± 0.05	0.07
PEEK Triangle- Weak Configuration	0.02 ± 0.005	0.07
PEEK Square	0.24 ± 0.14	0.15
Polyester .010" Triangle Wide Cross Section	0.89 ± 0.16	0.67
Polyester .010" Triangle Wide Cross –Weak Configuration	0.36 ± 0.13	0.67
Acrylic with PEEK Skin	4.15 ± 1.67	3.97
Polyester .010" Square wide	1.30 ± 0.11	1.46
Polyester .005" Triangle	0.13 ± 0.02	0.07
Polyester .005" Triangle Weak	0.03 ± 0.01	0.07
Polyester .010"Triangle	0.37 ± 0.02	0.13
Polyester .010" Triangle- Weak Configuration	0.088 ± 6.3e-04	0.13
3D Printed Square	11.7 ± 8.05	1.92
3D Printed Square Configuration 2	5.20 ± 1.50	1.92

Table 1: Results from the three-point bending tests. For the experimental stiffness EI, each beam was tested three times, and the average EI with 95% uncertainty interval was reported. EI was

also calculated using known values of Young's modulus E, and the respective formula for area moment of inertia I depending on the cross-sectional geometry. As expected, the acrylic with PEEK skin and the 3D printed beams had the highest stiffness values.

As we expected, the acrylic skeleton with PEEK skin had the highest stiffness value of the printable beams. It is comparable to the weaker configuration of the 3D printed beams. Generally the theoretical values for EI were consistent with what we experimentally measured, with a few exceptions. These could be due in part to problems with our experiment setup, such as accidentally plastically deforming a beam when applying the load or human error in loading the samples consistently. It is helpful to know that the theoretical values for EI are a decent approximation for the behavior of small scale, folded beams.

It is also important to note that the triangular beams have two loading configurations. There is one loading configuration where the tab and slot features are at the top (the face where the load is applied), which significantly decreases its stiffness. Possible solutions for this would be to have smaller tab and slot features more frequently along the length of the beam, reducing the areas with the long slits that decrease beam stiffness. Tab and slot features, especially with the thicker polyester can be time-consuming to fold by hand, so this is an important trade-off consideration.

We also noticed that the 3D printed beams have a weak and strong configuration based on the way the material was layered by the printer.
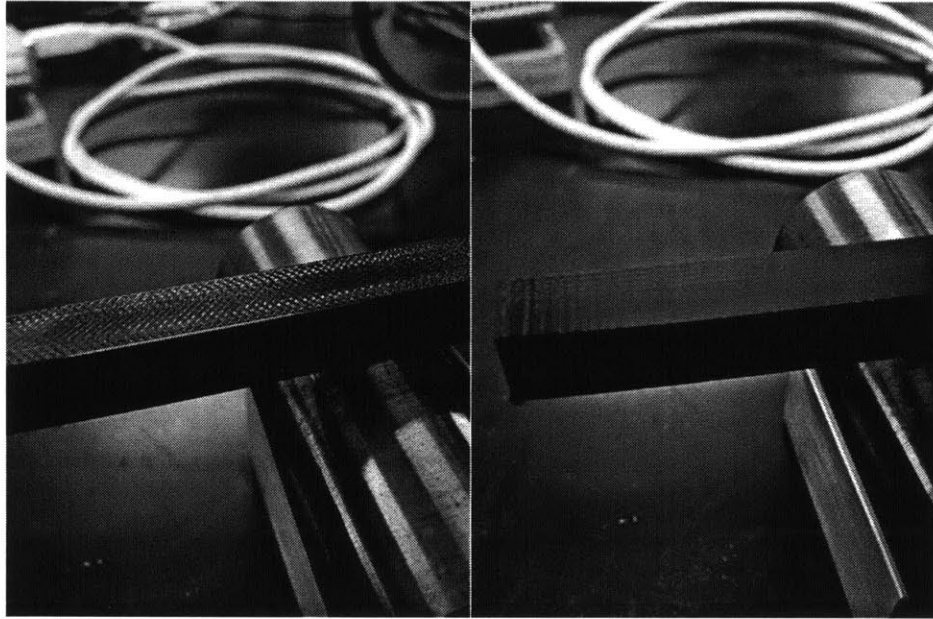
Figure 4 : Left) First and stronger configuration of the 3D printed beams, going with the layers of printed ABS. Right) The weaker configuration, going against the ABS layers.

Specimen	Time manufacture [s]	Time fold [s]	Weight [kg]
Polyester .005"	332	99	0.003
Polyester .010"	245	223.5	0.007
PEEK .005"	125	130	0.0035
Acrylic with PEEK skin	2820	600	0.086
3D printed beam	241.25	N/A	0.023

Table 2: An overview of the average time to manufacture (laser cut or 3D print) each type of beam, as well as the time to fold each type by hand. The thicker polyester is more time-consuming to fold, especially at small sizes. Also the weights of each type of beam are included

for comparison. In the printable robotics project, materials properties are not the only considerations when making design choices.

CONCLUSIONS

Knowing the beam stiffness EI for printable robots gives further insight into the properties and capabilities of these robots. This information will also be useful for the development of the printable robot compiler. It will also help make more informed design choices in future designs.

Overall we can see that the theoretical values for beam stiffness are generally similar to what we measured experimentally. This information is useful because it means we can trust standard analytical methods for predicting the behavior of simple structure designs. More complicated geometries might require further testing, especially as we discovered how the triangular cross-section beams had a weaker and stronger configuration.

REFERENCES

[1] C.D. Onal, R.J. Wood, and D. Rus, "An Origami-Inspired Approach to Worm Robots," IEEE/ASME Transactions on Mechatronics.
[2] Roylance, David. "Beam Displacements," Course Materials, Department of Materials Science and Engineering, MIT. 30 November 2000.
[3] Engineering Fundamentals, "Cross-Sections of Common Beams," eFunda, http://www.efunda.com/about/about.cfm. 06 May 2013.

[4] Totalcomp Documention, "TS 26 S-type Load Cell." http://totalcomp.com/ts25-p-661.html

[5] Measurement Computing Documention, "USB 1608fs." http://www.mccdaq.com/

[6] Kemmish, David, "Update on the Technology and Applications of PolyArylEtherKetones" 2010.

[7] MIT 3.11 Course Materials, http://web.mit.edu/course/3/3.11/www/modules/props.pdf